Reactive wetting in metal–metal systems

2009 J. Phys.: Condens. Matter 21 464130

(http://iopscience.iop.org/0953-8984/21/46/464130)

J. Phys.: Condens. Matter **21** (2009) 464130 (11pp) doi:10.1088/0953-8984/21/46/464130

Reactive wetting in metal–metal systems

Liang Yin[1], Bruce T Murray[1], Shun Su[1], Ying Sun[1], Yael Efraim[2], Haim Taitelbaum[2] and Timothy J Singler[1]

[1] Department of Mechanical Engineering, State University of New York, Binghamton, NY 13902-6000, USA
[2] Department of Physics, Bar Ilan University, Ramat-Gan, Israel

E-mail: singler@binghamton.edu

Received 18 June 2009, in final form 25 August 2009
Published 29 October 2009
Online at stacks.iop.org/JPhysCM/21/464130

Abstract
Wetting and spreading in high temperature reactive metal–metal systems is of significant importance in many joining processes. An overview of reactive wetting is presented outlining the principal differences between inert and reactive wetting. New experimental evidence is presented that identifies an early time regime in reactive wetting in which spreading occurs without macroscopic morphological change of the solid–liquid interface. This regime precedes the heavily studied reactive wetting regime. Additional new experimental evidence is presented of kinetic roughening in a high temperature reactive system. Quantitative characterization of this roughening reveals similarities with room temperature systems. These new data provide evidence that supports the existence of several sequential time regimes in the reactive wetting process in which different physicochemical phenomena are dominant.

(Some figures in this article are in colour only in the electronic version)

1. Overview

Reactive wetting is a subset of the heavily studied phenomenon of wetting, a process in which a liquid displaces another fluid on a solid substrate [1]. This process involves an advancing contact line, the dynamics and kinetics of which have comprised one of the long-standing fundamental problems in fluid physics. The majority of studies have focused on inert material systems in which the fluids do not react chemically with the solid substrate. The more limited study of reactive wetting has been inspired largely by industrial processes involving material systems in which the liquids react chemically with the solid [2]. Historically, the industrial processes of metallurgical joining have provided much of the impetus to the study of reactive wetting, most significantly soldering processes in microelectronics fabrication. These applications involve the wetting of metallic substrates by molten metal alloys. However, reactive wetting is not confined to inorganic material systems. Emergent technologies such as inkjetting and stamping of functional organic and biological materials is proving to be fertile ground for reactive wetting. For example, the initial capillary-driven spreading in wet stamping of alkane thiols and disulfides on gold has been observed to be extended by the subsequent formation of self-assembled monolayers [3]. Such emergent technologies will serve to diversify the interest in reactive wetting and elevate its intrinsic scientific merit.

It is worth delineating the distinction between wetting and spreading. Wetting, as described above, is really a process very local to the contact line region. Spreading is a macroscopic process and is generally understood to mean the global flow response of a liquid mass in contact with a solid substrate to a set of forces including capillary forces; this response necessarily involves the motion of a free surface and contact line. In inert systems, this global response leaves the solid–liquid (S/L) interface materially and morphologically unchanged. However, in reactive systems, the S/L interface undergoes complex material and morphological changes during spreading. Depending on the level of reactivity of the system, these changes can exert negligible to first-order effects on the wetting/spreading.

Whereas wetting in inert systems has been studied in the context of both forced and spontaneous wetting, reactive wetting has been studied almost exclusively via experiments utilizing spontaneous wetting. This is because the industrial applications that drive the interest in reactive wetting require that the material systems involved manifest intrinsically high wettability for optimal spontaneous wetting. Because of their simplicity, experiments employing both sessile and pendant drops have been used extensively to study spontaneous reactive

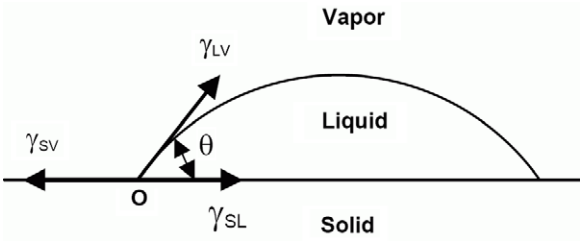

Figure 1. Schematic of inert wetting.

wetting. The essential aspects of wetting and spreading are thus discussed below from the perspective of spontaneously wetting drops.

1.1. The contact line region

In inert wetting systems, the contact line (CL) region is comparatively simple. The region is characterized geometrically by the dynamic contact angle θ_D, defined as the angle in the liquid formed between tangents to the liquid–vapor (L/V) interface and the S/L interface intersecting at the CL (figure 1). The interfacial tensions remain unchanged during the wetting process. The tendency to wet in such systems is predicted by the spreading coefficient $S = \gamma_{S/V} - \gamma_{S/L} - \gamma$, where $\gamma_{S/V}$ is the solid–vapor (S/V) interfacial energy, $\gamma_{S/L}$ is the solid–liquid interfacial energy and γ is the liquid–vapor (L/V) interfacial energy. For dynamic spreading (non-equilibrium), material systems for which $S < 0$ partially wet the solid substrate and form a non-zero equilibrium contact angle θ_E given by Young's equation $\gamma_{S/V} = \gamma_{S/L} - \gamma\cos\theta_E$. Systems for which $S = 0$ wet the substrate completely, forming a thin film of liquid for which $\theta_E = 0$. In either case, the CL moves under a given set of forces, which in spontaneously wetting systems must include the uncompensated Young force $F = \gamma_{S/V} - \gamma_{S/L} - \gamma\cos\theta_D = \gamma(\cos\theta_E - \cos\theta_D)$ normal to the contact line in the plane of the (undeformed) solid. It is implicitly assumed here that the interfacial energies have their equilibrium values so that S cannot be positive. However, if the solid surface is dry and its energy not lowered by the adsorption of the liquid's vapor, the resulting value $\gamma^0_{S/V}$ can be $O(10^2)$ larger than $\gamma_{S/V}$ and $S > 0$. Positive values of S are generally assumed to also yield perfect wetting.

For reactive metal–metal systems, the interaction between the liquid and solid can alter the contact line region whose geometry is then characterized by two angles θ_1 and θ_2 defined, respectively, as the angle in the liquid formed between tangents to the L/V interface and the original S/V interface intersecting at the CL and the angle in the liquid formed between tangents to the S/L interface and the original S/V interface intersecting at the CL (figure 2(a)). One of the fundamental difficulties, from the perspective of experiment, is that the high temperature reactive wetting environment is generally incompatible with standard measurement probes, and as a consequence temperature, composition, interface position and velocity information are lacking. A direct consequence of this limitation is a lack of data for the evolution of the S/L interface and, in particular, for the actual contact angle $\theta_L = \theta_1 + \theta_2$. Investigators have typically sought to explain reactive wetting, and more generally wetting in which there is phase change at the CL [4, 5], in terms of two observables, the wetted radius of the molten drop r and the superficial contact angle θ_1.

The driving force for reactive wetting is more complicated than for the inert case, in large part due to the end equilibrium state being difficult to determine and in some cases non-existent. True chemical equilibrium, as discussed below, takes years and is inaccessible by practical experiment. However, a quasi-equilibrium state often exists and corresponds to the sensible cessation of wetting, and one can pose a driving force in terms of this state. The actual CL configuration in reactive wetting depends on the nature of the reaction at the S/L interface at the contact line. As two examples, we consider the case of a purely dissolutive system and a compound forming system. Figure 2(a) shows the case of a purely dissolutive system in which a pure molten liquid A is placed on a pure solid substrate B. We consider a system in which the solubility of B in A is assumed much greater than the solubility of A in B, a specific example of which is the Bi–Sn system. During spreading, dissolution of B into A forms a solution AB in which gradients of concentration exist (such gradients can lead to non-uniform L/V interfacial energy if the substrate species is tensioactive; this is discussed below). Spreading continues and all interfacial quantities vary with time. Continued dissolution and mass transport makes the solution more homogeneous and concentration gradients weaken. In the contact line region, the solution can become saturated in which case wetting occurs without significant additional dissolution. In this case, $\theta_2 \to 0$ and wetting stops when $\theta_1 = \theta_E$ (figure 2(b)). The wetting force can then be written $F = \gamma_{S/L}(t)[\gamma_{S/L}/\gamma_{S/L}(t) - \cos\theta_2(t)] + \gamma_{L/V}(t)[\gamma_{L/V}/\gamma_{L/V}(t)\cos\theta_E - \cos\theta_1(t)] - \Delta G(t)$,

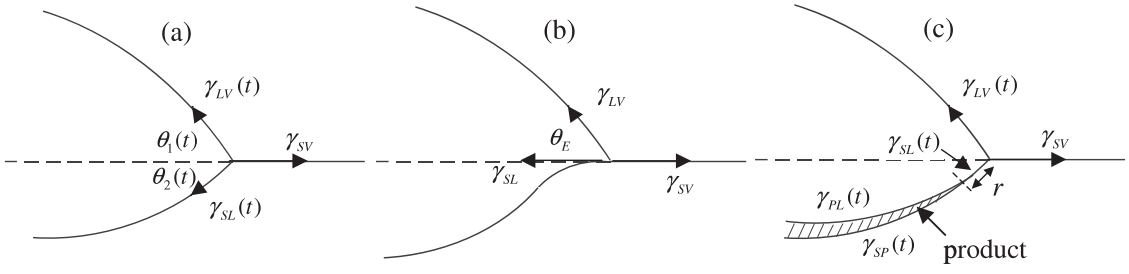

Figure 2. Schematics of dissolutive and compound forming wetting systems.

where $\Delta G(t)$ is the change in the Gibbs free energy released by the dissolution reaction.

Figure 2(c) shows the case of a compound forming system. Let us again consider a pure molten liquid A placed on a pure solid substrate B. A reacts with B to form A_xB_y and we again assume that the solubility of B in A is much greater than the solubility of A in B, a specific example of which is the Au–Sn system at 280 °C which forms the ϵ-phase $AuSn_2$. The intermetallic A_xB_y lags the CL by a distance r; Boettinger *et al* [6] first noted that intermetallic may not form at the CL because of a local inability to overcome the nucleation barrier on timescales corresponding to rapid to modest CL speeds. At first glance, then, the CL configuration appears as in figure 2(a); however, the equilibrium state is not the same. As the system approaches equilibrium, the CL slows and $r \to 0$: the slower speed allows nucleation to occur. When the reaction product serves as an effective diffusion barrier on the timescale of wetting, the quasi-equilibrium state $\theta_1 = \theta_{1,E}$, $\theta_2 = \theta_{2,E}$ and $\theta_P = \theta_{P,E}$ can occur, where θ_P is the angle between the liquid/product interface and the product/solid interface at r. The driving force may then be written in terms of this equilibrium as $F = \gamma_{S/L}(t)[\gamma_{L/P}/\gamma_{S/L}(t)\cos\theta_{2,E} - \cos\theta_2(t)] + \gamma_{L/V}(t)[\gamma_{L/V}/\gamma_{L/V}(t)\cos\theta_{1,E} - \cos\theta_1(t)] + \gamma_{S/P}(t)[\gamma_{S/P}/\gamma_{S/P}(t)\cos\theta_{P,E} - \cos\theta_P(t)] - \Delta G(t)$, where $\Delta G(t)$ is the change in the Gibbs free energy released by the dissolution/compound-formation reaction. However, in some metal–metal systems (e.g. Au–Sn at 250 °C), the growth of the intermetallic compound pervades the CL region, i.e. $\theta_2(t) \to -\theta_1(t)$ on the timescale of wetting. Thus the contact line arrests due to solutal freezing and there is no effective end equilibrium state. There are other possible configurations of the CL region which would manifest different forces. But as noted above, there has been little or no direct experimental confirmation of the S/L phase boundary dynamics. However, in the following section, we present novel experimental observations of the S/L boundary in a metal–metal system by using a variation of the Hele–Shaw cell (described in detail below).

The above discussion assumes that the CL remains in the plane of the original S/V interface. There have been some reports of the reaction product forming ahead of the contact line [2]. This seems to primarily occur in spreading on ceramic substrates in which case the reaction product is assumed to be extremely thin and to negligibly displace the CL upward. Dussan [7] questioned the effect of the vertical component of surface tension on the contact line, suggesting a reaction force in the solid (and raised the question why such a reaction should only have a vertical component!). In inert systems, this leads to an elastic deformation of the S/L boundary that relaxes on passage of the CL. In reactive systems, however, mass transport affords a mechanism by which the deformation may grow, culminating in a CL ridge [8, 9] whose kinetics may control the CL motion in some systems. This fundamental consideration may be avoided in metal–metal systems as dissolution provides a vertical component of S/L interfacial tension that may be assumed to balance the vertical L/V tension component.

The force F leads to motion of the contact line that is resisted by viscous forces. The resulting kinetics of the CL are often described in terms of a relationship between the CL speed and the contact angle. We defer discussion of this relationship to section 1.2.

1.2. The solid/liquid interface

Experimentally, the real-time S/L interface in high temperature metal–metal systems is refractory to conventional probes. The majority of the data regarding the evolution of the S/L interface are based on post-mortem analysis of solidified wetting samples (cf, [10, 11]) or theoretical predictions based on assumptions designed to yield a more tractable model. This is unfortunate because the dynamics and evolution of the S/L interface really form the crux of the reactive wetting problem. Whereas in inert wetting/spreading the S/L interface remains unaltered, the chemical and morphological changes of the S/L interface occurring for reactive wetting can be very dramatic. For example, in the purely dissolutive Sn–Bi system, a given volume of Sn can dissolve over 3.5 times its volume of Bi at 250 °C, resulting in a deep dissolution well under the wetted area of the initially flat S/L interface [10, 12]. The S/L interface evolution for compound forming systems is significantly more complex because of the varied behavior of different material systems. Even for a given system, the compounds that form at different temperatures can influence the dynamics of wetting and spreading in very different ways. Consider the Au–Sn system as an example. Yin *et al* [11] showed that at 250 °C, the solubility of Au in Sn is limited (∼90 at.% Sn), and dissolution effects are modest. Between 500 and 600 s from initiation of wetting, η-phase ($AuSn_4$) intermetallic compound begins to form in the CL region and coexists with the saturated liquid phase. The percentage of compound in the CL region increases until the CL motion is arrested by isothermal solidification.

The effect of compound formation at the S/L interface is not limited to CL arrest. Away from the CL region, compound formation at the S/L interface can mediate the transport of Au into the liquid drop. A suggested path for compound formation entails heterogeneous nucleation on the S/L interface with a certain amount of super-saturation in the liquid phase to overcome the nucleation energy barrier. Once a continuous layer of intermetallic compound forms at the S/L interface, transport of Au and Sn must occur through the layer by solid-state diffusion, i.e. volume diffusion and grain boundary diffusion, which probably substantially reduces the rate of substrate dissolution. An estimate for the diffusivity $\mathcal{D}_\eta$ of Au in $AuSn_4$ is $\mathcal{D}_\eta \sim 3.2 \times 10^{-7}$ cm^2 s^{-1}. This value is two orders of magnitude smaller than the diffusivity of Au in liquid Sn, $\mathcal{D}_L \sim 1.6 \times 10^{-5}$ cm^2 s^{-1}.

The growth of compounds at the S/L interface is not always confined to thin layers that attenuate the dissolution of solid. In the temperature range 315–415 °C, the δ-phase (AuSn) intermetallic grows very rapidly at the initiation of wetting, causing solidification of a substantial amount of liquid throughout the drop; with further dissolution the intermetallic reverts to a liquid phase in the form of a Au-rich liquid. This solid → liquid → solid phase transition occurs in less than 350 ms at 315 °C. The comparatively rapid kinetics of the δ-phase intermetallic were previously

unreported in the literature, a fact that underscores the difficulty in identifying the role played by the S/L interface in reactive wetting/spreading.

1.3. The liquid/vapor interface

Liquid metals have the largest surface tensions of any class of liquids. The use of both sessile and pendant drops to assess wetting performance in metallic material systems implies that gravity and surface tension have antagonistic roles for sessile drops and synergistic roles in pendant drops. The relative effects of gravity and surface tension are estimated by the Bond number $Bo = L^2/L_c^2$ where L is a characteristic length scale of the liquid phase and $L_c \equiv (\sigma/(\rho g))^{1/2}$ is the capillary length in which σ is the surface tension, ρ is the liquid density and g is the acceleration of gravity. When $Bo \ll 1$, the effect of gravity on the pressure distribution within the drop is negligible; this is tantamount to assuming that the drop has constant curvature and that the pressure within the drop is constant. This further implies that the drop is driven by an uncompensated Young force (inert wetting) and additional thermodynamic reactive forces (reactive wetting). For example, for pure tin at 250 °C, $Bo = 1.4 \times 10^{-2}$. In continuum computational studies of the reactive Sn–Bi system [13, 14], the L/V interface has been constrained to be a spherical cap. In these studies, the Sn–Bi solutions were assumed to be ideal and thus had zero volume of mixing. Under the constraint of fixed liquid volume, the superficial contact angle θ_l can be calculated by simple geometry knowing the wetted radius of the drop. However, the asymptotic limit $Bo \to 0$ provides a good approximation to the global interfacial shape but this approximation is not valid near the contact line where large hydrodynamic forces induce a deviation from constant curvature. Most careful reactive wetting experiments measure the contact angle directly. This is possible up until the point that phase change occurs in the CL region and a solid phase introduces uncertainty in the position of the CL; this occurrence is conjectured to be associated with the onset of the kinetic roughening regime. However, the global constant curvature approximation is still useful experimentally to assess the level of oxidation: most experimentalists look for the appearance of a spherical cap during wetting to confirm minimal presence of oxides on the L/V interface.

The well-known dependence of surface tension on temperature T and concentration C provides for the possibility that L/V interfacial gradients in these physicochemical variables induce thermo- and soluto-capillary effects, respectively. The role of thermocapillarity in spreading drops was analyzed by Erhardt and Davis [17]. They found that, for drops spreading on substrates whose temperature was greater than that of ambient atmosphere, thermocapillarity induced a L/V interfacial flow from the CL to the drop apex; this thermocapillary flow inhibited wetting. Conversely, they found that for drops spreading on substrates whose temperature was less than that of ambient atmosphere, thermocapillarity induced a L/V interfacial flow from the drop apex to the CL; this thermocapillary flow enhanced wetting. These results apply equally to the sessile and pendant drop configurations.

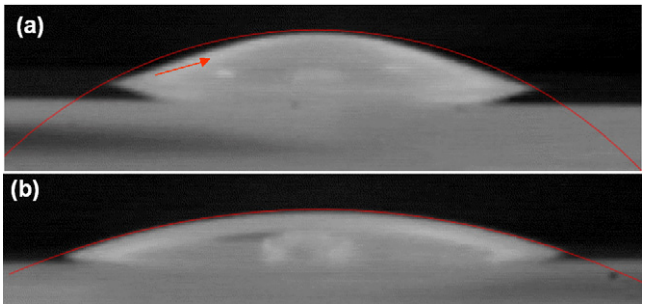

Figure 3. Deformation effects of soluto-capillary flow in the Cu–Si system. (Figure contributed by Protsenko *et al* [18].)

In high temperature capillarity experiments, it is almost always the case that the substrate temperature exceeds that of the ambient atmosphere and so thermocapillary effects would be inhibitive of wetting; however, temperature differences are unlikely to be large enough to drive significant thermocapillary motions.

Soluto-capillary effects are much more likely to influence wetting in metal–metal systems when the substrate metal is strongly tensioactive. For example, in the Cu–Si system, pure Cu has a surface tension of approximately 1280 mN m^{-1} while the surface tension of a saturated Cu–Si solution at 1100 °C is 840 mN m^{-1}. When the reactive wetting regime is reached, as a first-order approximation, one may assume that due to dissolution the concentration of Si at the CL is that of a saturated Cu–Si solution and that at the drop apex is zero (still pure Cu). The resulting soluto-capillary flow on the L/V interface is then from CL to drop apex and wetting is inhibited. The resulting mass transport due to viscous coupling between the L/V interfacial liquid and bulk liquid in the drop depletes liquid in the CL region and accrues liquid at the apex. Figure 3 shows the Cu–Si system for both a pure Cu drop and a saturated Cu–Si drop, wetting pure Si. In the former case, a strong soluto-capillary effect exists and the liquid distribution as described above is clearly evident; in the latter case, no dissolution occurs, the distribution of tensioactive solute (Si) is uniform, and therefore no soluto-capillary effects are present. The images are both at 50 ms from the initiation of wetting and the wetted radius r for the former case is significantly smaller than for the former, clearly illustrating the retardation of wetting by the adverse soluto-capillary flow.

2. Four stages of wetting in metal–metal systems

In this section, we assert that there are generally four sequential stages of wetting in metal–metal systems: (1) a very early time regime in which the liquid spreads with no discernible morphological change of the S/L interface; (2) a highly reactive regime in which reaction exerts a first-order effect on the wetting/spreading and during which significant morphological and chemical changes of the S/L interface can occur; (3) a kinetic roughening regime characterized by growth of a solid phase in the contact line region which roughens an otherwise smooth contact line; (4) a very late time regime when the wetting specimen's interfaces equilibrate by solid-state diffusion.

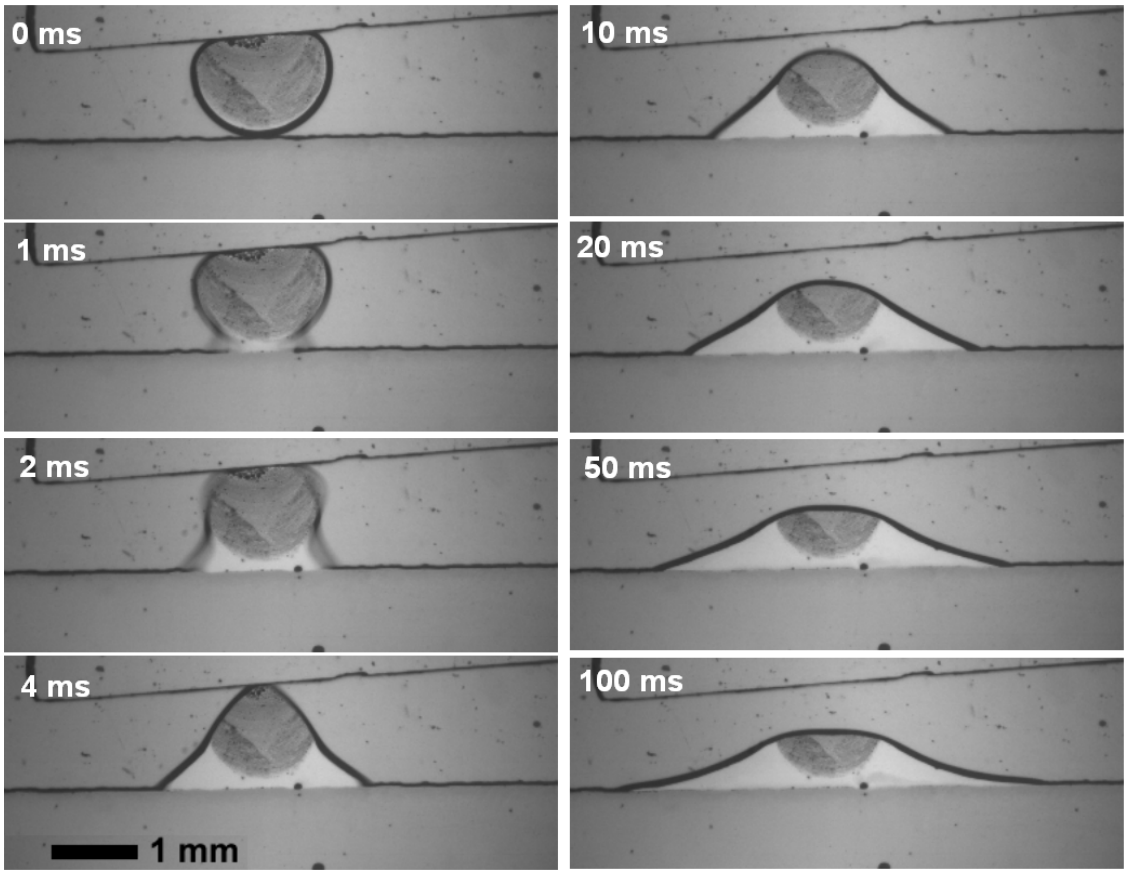

Figure 4. Images of a pure Sn drop wetting pure Bi in a Hele–Shaw cell. The images were acquired using high speed motion analysis at 1000 frames/s.

2.1. Early time regime

There has been some speculation that during the initial stages of wetting initiated by drop transfer the liquid metal spreads on the metal or ceramic substrate with no chemical interaction with the substrate thus leaving the S/L interface in its original flat unreacted state. This phase of wetting has in some cases been referred to as 'inert' wetting. However, until this time, there really has been no experimental or theoretical substantiation of this claim. Of course the main reason for this lack of justification, as noted above, is the dearth of real-time observations of the S/L interface evolution. Yin *et al* [15] introduced a new reactive wetting environ by performing high temperature wetting experiments in transparent Hele–Shaw cells. Hele–Shaw cell involves the flow of a fluid between two parallel flat plates, which are fixed at a small distance h apart [16]. The narrow-gap geometry and transparent cell walls enabled the real-time observation of the evolution of both the L/V and S/L interfaces. The proof-of-concept experiments were followed by improved experiments[3], the results of which are shown below, in which the dynamics of the interfaces were recorded using both high speed videography and higher resolution video.

Experiments were performed for the Bi–Sn system at 250 °C. Figures 4 and 5 show results for an initially pure Sn drop wetting a pure Bi substrate. The gap width h is 225 μm and the mass of the Sn drop 2.5 mg, which gave an approximate drop diameter d of 1.4 mm (the shape of the drop in this geometry is a disk with a sharply curved edge due to capillary effects); this gives a Hele–Shaw parameter $\epsilon \equiv h/d = 1.6 \times 10^{-1}$. Figure 4 shows selected images from a high speed recording of a wetting event. From this high speed sequence it may be seen that no morphological change of the S/L interface is apparent through the first 100 ms, i.e. the S/L interface remains macroscopically flat. The maximum CL speed $U_{\mathrm{CL_{MAX}}} = 0.65\ \mathrm{m\ s^{-1}}$ occurs in the first few seconds of wetting. This initial speed gives a capillary number $Ca \sim 2 \times 10^{-3}$ (which subsequently decreases monotonically with time); theoretical analysis for $Ca \ll 1$ predicts that the L/V interface under the action of capillary pressure gradients first tries to become circular (contact line push) and then under the action of an unbalanced Young force tries to spread as a circular section (contact line pull) [19].

In the present experiments, the attempt of the L/V interface to achieve circularity was mildly frustrated by the presence of Sn oxide (the dark region on the glass–Sn interface in figure 4). The formic acid vapor used to control oxides in the experiment was established to be effective for the Sn–Bi system in an open geometry [11], but the closed Hele–Shaw geometry limits transport of the vapor to the interface. In the present experiments, since most of the oxide remained

[3] See Yin *et al* [15] for details of the original experiments; details of the improved experiments will be presented in a forthcoming paper.

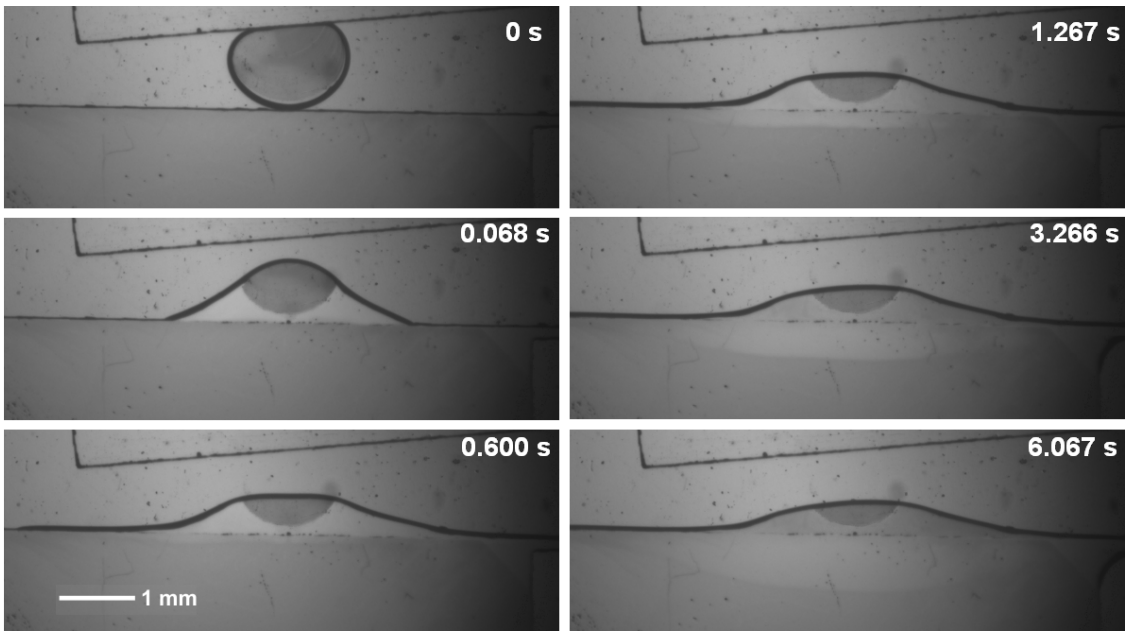

Figure 5. Images of a pure Sn drop wetting pure Bi in a Hele–Shaw cell. The images were acquired using a high resolution camera 15 frames/s.

on the glass–Sn interface, its influence was not catastrophic. Figure 4 shows selected frames from high speed videography (512 × 384, 1000 frames/s) that reveal that the S/L interface does not undergo macroscopic morphological change through the first 100 ms of spreading, i.e. the S/L interface remains flat. Figure 5 shows an identical spreading event comprising a sequence of images from a camera system (2448 × 2050, 15 frames/s) with a greater frame storage capacity. It reveals that the onset of morphological change of the L/S interface due to dissolution occurs at approximately 600 ms from the initiation of wetting. The L/S interface is demarcated by the line separating darker gray (pure Bi solid) and lighter gray (Bi–Sn liquid) below the original flat interface. Subsequent frames (with time stamps of 1.267, 3.266 and 6.067 s) show that the L/S interface continues to evolve, advancing laterally with increase of the wetted radius r and more deeply into the solid Bi. Although the sequence does not extend to the cessation of wetting associated with a quasi-equilibrium state, it is clear that, as in the Bi–Sn open-geometry sessile drop experiments of Yin *et al* [11], a volume of Bi is dissolved that is significantly greater than the original volume of the Sn drop. The evolution of the S/L interface also has similarities to the sessile drop experiments [11] and to continuum computational predictions [13, 14] for the Bi–Sn system: at the onset of morphological change (600 ms) the interface tends to be flat, and with increasing time tends to become circular. But as noted above, the current reactive wetting experiments were conducted in a novel geometry for which no theoretical or computational models yet exist. The potential value of the current geometry in helping to elucidate the dynamics of S/L interface evolution warrants the development of such models.

Figures 4 and 5 together provide the first real-time visual evidence that an early time regime can exist for reactive metal–metal systems during which spreading can occur with no macroscopic alteration of the originally flat S/L interface. Some speculative claims about this regime refer to the wetting as inert. We emphasize that the above results do not validate this claim. Based on the discussion in section 1.1 above, inert wetting would correspond to $\Delta G(t) = 0$ so that no thermodynamic component to the driving force at the CL exists. However, it is likely that even for a very reactive system, the non-zero $\Delta G(t)$ associated with CL advance must derive from an interaction with the solid substrate that involves a microscopic volume. Thus one cannot infer from a macroscopically unaltered L/S interface during spreading that the wetting is inert.

An additional comment on this regime is in order. The early time regime will not be observed for all experimental techniques for delivery of the liquid metal to the reactive substrate. In the case of placement of a solid sphere on a pre-heated substrate, liquid is made available to the spreading process on the timescale for melting of the sphere, i.e. the thermal diffusion timescale $t_m \sim d^2/\kappa$, where d is the sphere diameter and κ is the thermal diffusivity; for Sn spheres at 250 °C, $t_m \sim 96$ ms. Therefore, the early time regime appears to occur only for liquid delivery techniques.

2.2. Reactive wetting regime

This regime is one in which the reaction exerts a first-order effect on the wetting/spreading. The preponderance of the literature on reactive wetting focuses on this regime and we shall not attempt to provide a detailed discussion or review; we merely mention several salient aspects of this regime pertinent to the theme of the paper. We note that even the simplest case of reactive wetting in metal–metal systems, when the reaction consists solely of dissolution, is not yet fully understood. Reactive wetting involving compound

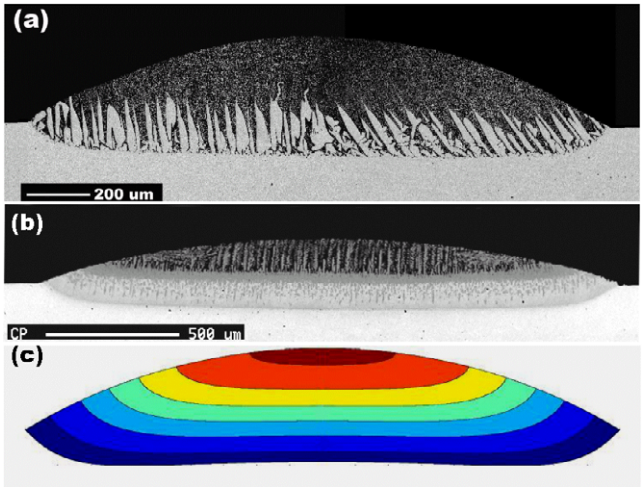

Figure 6. Experimental isoconcentrates for (a) eutectic Bi–Sn alloy wetting pure Bi at 250 °C, (b) pure Sn wetting pure Au at 430 °C. Computational isoconcentrates for (c) 80Bi20Sn alloy drop wetting pure Bi at 250 °C.

formation presents significantly more formidable barriers to understanding.

A reasonably good picture has been developed of the mass transport within the drop for a purely dissolutive system. This picture has come from a combination of experiment and continuum computations. Computational studies usually assume that an initial state exists in which the pure liquid metal (or alloy of given composition) already exists on the unreacted solid in the shape of a partially spread drop. In some senses, the end of the early time regime provides an initial condition of precisely this nature. Evolution of drop spreading is computed from the continuum equations from this initial state. Continuum computations have been performed for the Bi–Sn system and these are qualitatively representative for any purely dissolutive system with large solubility and possibly for some reactive systems at temperatures at which the solubility is large. A primary representation of the computed concentration field from these calculations has been the isoconcentrates, because the demarcation between phases of solidified spreading specimens actually visualizes critical isoconcentrates.

Figure 6 exhibits isoconcentrates from experiment and computation. Figure 6(a) reveals an isoconcentrate of a eutectic Bi–Sn alloy drop wetting pure Bi at 250 °C after quenching at 3 s. Figure 6(b) shows two isoconcentrates of a pure Sn drop wetting pure Au at 430 °C (at which temperature there is a very large solubility of Au in Sn) after quenching at 1.5 s. Figure 6(c) shows a computed concentration contour plot of an 80Bi20Sn alloy drop wetting pure Bi at 250 °C. The shapes of contours from both experiment and computation are similar. In the computational model, the boundary conditions imposed at the L/V and S/L interfaces determine the macroscopic value of the angle θ_L. A condition of zero flux is imposed on the solute at the L/V interface and this requires that isoconcentrates intersect the L/V interface at right angles. At the S/L interface, the condition of equilibrium, corrected for interfacial curvature (Gibbs–Thomson) is imposed. Because the multiplicative factor of the curvature in the correction is small and the L/S interface is regular, the interface behaves effectively as an isoconcentrate and intersects the L/V interface at a right angle. It is difficult to verify this prediction by experiment because the changes in interfacial shape during solidification are unknown, but the experimental images do show a significant change in slope of the S/L interface in the predicted direction near the CL. It is interesting to note that an *ad hoc* value of θ_L much smaller than $\pi/2$ was imposed by Warren *et al* [13] and Su *et al* [14] at sub-macroscopic length scales which constrained the interfaces to meet at that angle; however, the macroscopic behavior of the S/L interface was such as to make $\theta_L \sim \pi/2$. Su *et al* [14] did explore using the experimentally obtained data for θ_L of Yin *et al* [11] and obtained better agreement with r versus t data than with *ad hoc* values. However, the data were obtained using rapidly quenched wetting specimens and the validity of the measured θ_L values remains questionable.

Considerable effort has been directed at finding a universal relationship between the dynamic superficial contact angle θ_l and the contact line speed U_{CL} (or capillary number Ca). The motivation for such study has been the existence of such relationships for perfectly wetting and partially wetting inert material systems [20]. These attempts have largely resulted in failure. In the case of inert systems it is well known that the $\theta_l(U_{CL})$ relationship results from the interaction of two forces, the uncompensated Young force at the contact line and the viscous dissipation in the CL region. Furthermore, the angle θ_l is the true contact angle. In the reactive case, in addition to the uncompensated Young force (itself ill-defined in reactive wetting) and viscous dissipation, both phase change and compound formation—and mass transport associated with these processes—can also be occurring in the CL region. Moreover, the true contact angle in the reactive case is θ_L, and not θ_l. With the identification of several regimes in this paper it is also possible that different sets of forces are emphasized in each. It seems doubtful, then, that a single relationship—such as exists for the inert wetting case—can faithfully represent the $\theta_l(U_{CL})$ behavior over the entire interval of wetting in which U_{CL} ranges from its maximum value to zero.

2.3. Kinetic roughening regime

Kinetic roughening is a term referring to the transition of a nominally circular CL and smooth L/V interface to an irregularly shaped CL and L/V interface. Roughening does not appear to be a CL instability but rather the growth of a new phase in the CL region. This phenomenon was originally identified by Taitelbaum and co-workers [22–24] who studied the room temperature wetting of Ag and Au coatings on glass by liquid Hg. These authors also considered different time regimes, related to those regimes being discussed here [25, 26]. Yin *et al* [15] looked at wetting of pure Sn on Au-coated Cu and observed dramatic roughening behavior that was very sensitive to temperature and dwell time of the substrate on the hot stage (the latter influenced the amount of Cu present on the S/V interface). A sequence of images from these experiments is shown in figure 7.

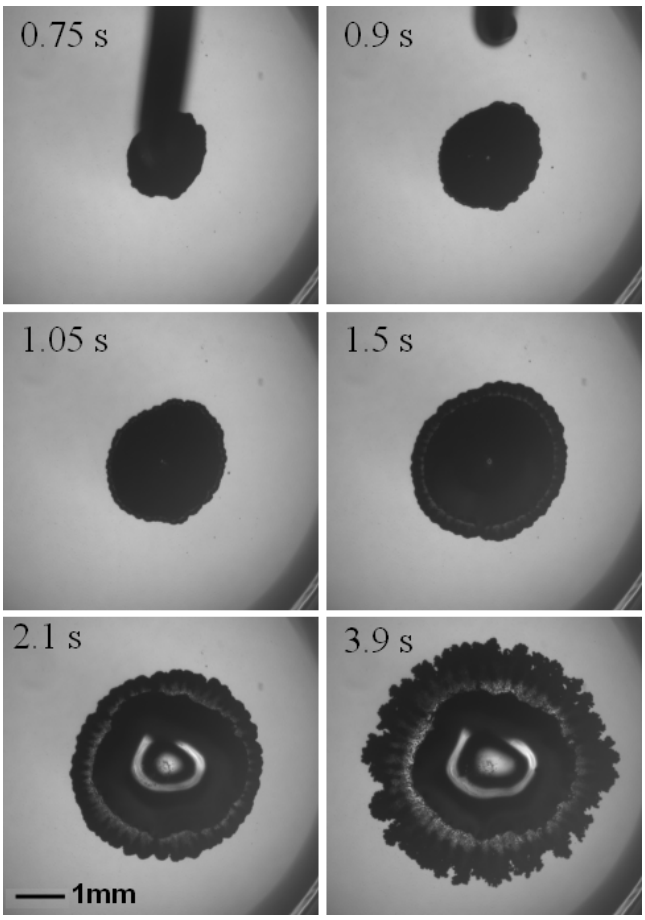

Figure 7. Kinetic roughening regime for pure Sn wetting a 1 μm Au coating over 12 μm Cu at 390 °C and a dwell time of 1 min.

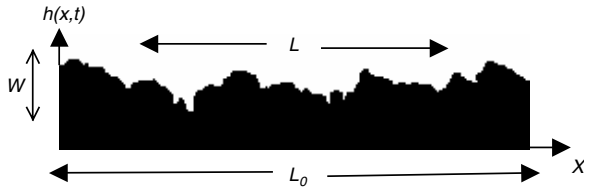

Figure 8. Illustration of an interface of length L_0 at a certain time.

The conditions that evolve in the reactive wetting regime that cause kinetic roughening are not at all understood. It was originally thought that thin films of substrate metallization were required to induce this phenomenon, but Yin *et al* [10] observed it in the Au–Sn system where the substrate thickness was effectively infinite. Furthermore, the Cu thickness in the experiments in figure 7 was also effectively infinite (observation of the back of the substrates through the glass slide on which the metallization was deposited revealed no indication that dissolution had pervaded the entire Cu layer). However, no observation of kinetic roughening has been reported for purely dissolutive material systems, so it appears that compound formation plays an essential role.

Below, we present initial studies characterizing kinetic roughening in a high temperature system, the wetting of Au-coated Cu by pure Sn.

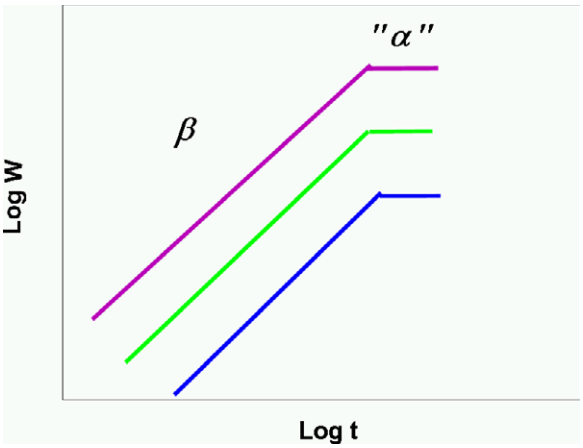

Figure 9. Illustration of $W(t)$ in log–log scale, as predicted by equation (2). A straight line with slope β that saturates after time t^*. After saturation the roughness exponent α can be measured. Different colored lines mark different window sizes L.

2.3.1. Short overview of the statistical analysis. The main measures that are used to study the irregularly shaped CL interface kinetics and geometry are the kinetic roughening exponents α and β. It is convenient to describe the interface as a function $h(x, t)$ that is simply the interface height as function of time and space. The second moment of $h(x, t)$ corresponds to the interface *width* at each time. One can calculate the second moment not only for the overall interface but also for different parts of it ('windows'), at size L. Hence W is a function of both time and 'window size' L,

$$W(L, t) = \sqrt{\langle h^2(x, t)\rangle - \langle h(x, t)\rangle^2} \tag{1}$$

where the angular brackets denote spatial average within the chosen 'window' L (see figure 8).

The Family–Vicseck relation [21] describes the asymptotic behavior of the interface width's at short times, when the interface is still growing, and at long times, when the interface width saturates as

$$W(L, t) \approx \begin{cases} t^{\beta} & t \ll t^* \\ L^{\alpha} & t \gg t^* \end{cases} \tag{2}$$

where the crossover time t^* is given by the system size L_0 and the two exponents as

$$t^* \propto L_0^{\alpha/\beta}. \tag{3}$$

According to this asymptotic scaling, if one plots $W(t)$ in a log–log scale, one should get a straight line with slope β, that after time t^* saturates, crossing to the regime where roughness can be measured (see figure 9).

β is the growth exponent which characterizes the time evolution of the interface, and α is the roughness exponent which describes the geometry of the interface after its width reaches saturation. On the basis of the roughness exponent one can calculate the lateral correlation length of an interface, which reflects collective behavior of points along the interface up to a certain length scale, L_x [22]:

$$C(L) = [\langle (h(x) - h(x'))^2\rangle_{x'}]^{1/2} \sim L^{\alpha} \tag{4}$$

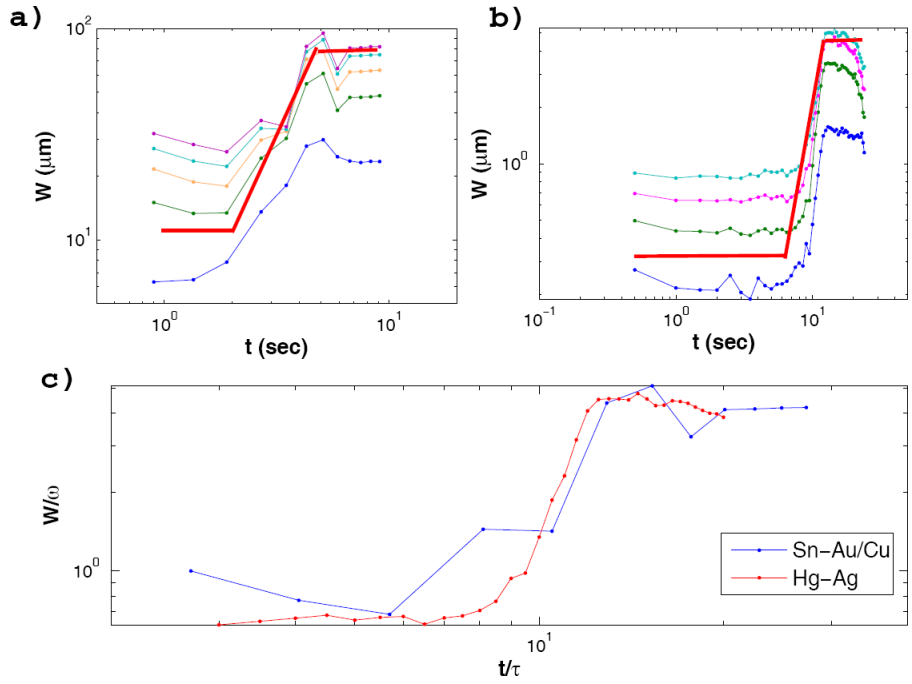

Figure 10. $W(t)$ of a single reactive wetting experiment in Sn–Au/Cu (a) and in Hg–Ag (b). The thick lines mark the trend in each time regime. A direct comparison with dimensionless parameters is presented in (c). The similar trend in both experiments indicates that the interface dynamics is not material dependent.

where $L = |x - x'|$. It was recently shown that it is also possible to calculate the correlation length on the basis of the dynamics of the interface, i.e. from the fluctuations of the interface width in time [22]. This indirect method which leads to the same length scale as obtained using the roughness exponent shows once again that the statistical calculation reveals relevant physical information. In addition, on the basis of the growth and roughness exponents one may be able to classify the system into a certain universality class that sheds light on the fundamental mechanisms in the process.

2.3.2. Results. A set of experiments of Sn droplets spreading on a 1 μm coating of Au on Cu of thickness 12 μm, deposited on glass, at temperature 390 °C was analyzed (for detailed information on the experimental setup see Yin *et al* [15]). When we plotted the interface width W as function of time, we recognized behavior similar to the Hg–Ag interfaces where one can define three different regimes of the interface dynamics [23] (see figures 10(a), (b)). Figure 10(c) presents a comparison between the Hg–Ag system and the Sn–Au/Cu system. Since both time and length scales are different in the two systems, we rescaled both the t and W axis. The scaling parameters τ and ω (for t and W, respectively) were found empirically to be $\tau_{\mathrm{Hg-Ag}} = 1$ s and $\tau_{\mathrm{Sn-Au/Cu}} = 1/3$ s; $\omega_{\mathrm{Hg-Ag}} = 1$ μm and $\omega_{\mathrm{Sn-Au/Cu}} = 15$ μm. This means that the process in the high temperature Sn–Au/Cu system is about three times faster than the room temperature Hg–Ag system. In addition, in the given experimental resolutions, 1 μm in the Sn–Au/Cu corresponds to 15 μm in the Hg–Ag system.

The first regime is where the interface advances but the growth is not starting yet, meaning that the interface width is approximately constant. For the Hg–Ag system we showed, using the persistence measure [23], that in this regime the main mechanism which drives the system is simply noise that causes minor fluctuations in the interface shape but not yet leading to effective growth of the interface width. The second regime is the growth regime, where the interface width grows according to the Family–Vicseck law (equation (2)), and the growth exponent β is defined. In order to properly calculate the growth exponent β, one should shift the time axis so that $t_g = 0$ corresponds to the start of growth (see figure 11). The growth exponent, which is the slope of the width versus the shifted time in log–log scale, was found to be $\beta = 0.62 \pm 0.039$. This result resembles the growth exponent that was found in the Hg–Ag reactive wetting system [24].

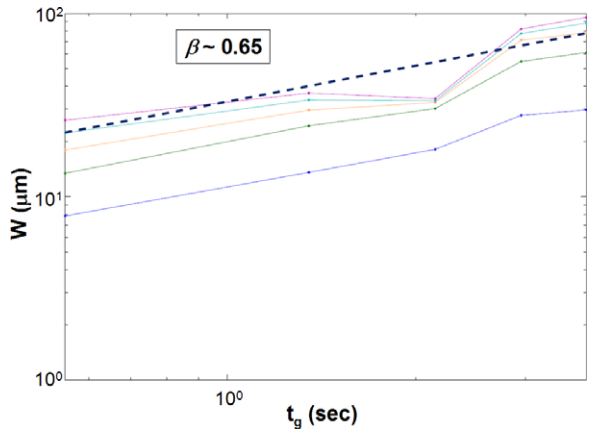

Figure 11. W as a function of the (shifted) time axis t_g for a single experiment in the Sn–Au/Cu system. The slope is the growth exponent β.

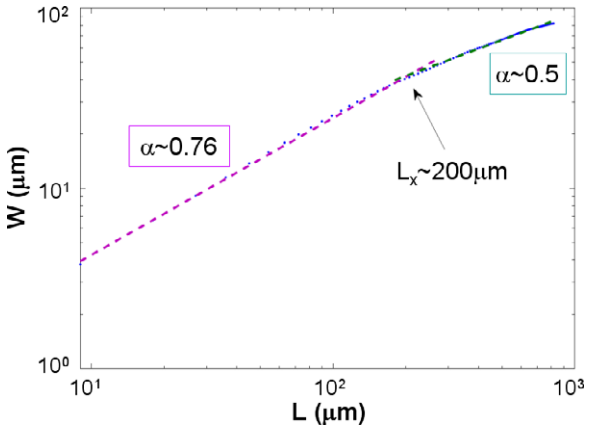

Figure 12. $W(L)$ in a single experiment in the Sn–Au/Cu system. It exhibits a straight line with slope $\alpha = 0.76$ that crosses over to a slope of almost 0.5 around $L_x = 200$ μm.

The last regime is where the interface saturates and the roughness exponent α becomes relevant. In this regime we are interested in the geometry of the interface, thus we plot the interface width as a function of length on a log–log scale (figure 12). According to the Family–Vicseck law (equation (2)) one should expect a straight line with slope that is the roughness exponent α. As shown in figure 12 for a single system, we do get a straight line which crosses over from an average slope of $\alpha = 0.77 \pm 0.00$ to 0.48 ± 0.02 which is approximately 0.5 (random roughness). The crossover occurs at $L_x = 171 \pm 36$ μm, and is interpreted as the lateral correlation length of the interface. This characteristic length scale indicates the range of collective behavior of points along the CL. Beyond this length scale, there is no correlation between distant points, and the kinetic roughening can be considered random. A similar crossover was also found in reactive wetting interfaces of a Hg droplet on Ag and Au substrates [22].

The similarity between reactive wetting experiments of different materials in various thicknesses can now be examined quantitatively on the basis of the kinetic roughening exponents α and β (table 1). One can see that the growth exponent of the system under study, Sn–Au/Cu, is very close to the growth exponent of Hg on thick Ag (lines 1–2). The value of the roughness exponent α is usually around 0.8. This variation around 0.8 can be caused by other effects, like overhangs [24]. Therefore, it seems that the Sn–Au/Cu belongs to the same universality class as the Hg–Ag system. According to the value of the exponents, we conjecture that this is the QKPZ universality class whose exponents are $\beta = 3/5$ and $\alpha = 3/4$ [21, 27]. The Hg–Au system belongs to a different universality class; however, it obeys the same hyper-scaling relation, as discussed in detail in [30].

2.4. Late time regime

The cessation of wetting, i.e. the sensible stopping of CL advance, that is observed in actual experiments is not associated with a true equilibrium but rather a quasi-equilibrium. From a practical perspective, the experiment is complete. However, the interfaces are not in equilibrium and will equilibrate by diffusion driven by curvature gradients along the S/L interface. Through a scaling analysis of the evolution equation, Yin *et al* [11] showed this equilibration to take years. This equilibration will result in changes to both L/V and S/L interface morphologies as well as wetted radius.

Table 1. Comparison of the kinetic roughening exponents α and β among various reactive wetting systems.

Reactive wetting systems	α	β
Hg on 4000 Å Ag [28]	0.67 ± 0.06	0.83 ± 0.00
Hg on 0.1 mm Ag (thick foil) [29]	0.60 ± 0.02	0.82 ± 0.04
Hg on 1500 Å Au [30]	0.76 ± 0.03	0.85 ± 0.03
Sn on a 1 μm coating Au on 12 μm Cu	0.62 ± 0.04	0.77 ± 0.00

3. Conclusions

The wetting and spreading of molten metal drops on solid metal substrates at elevated temperatures presents a complex reactive wetting system. Potential reaction mechanisms are dissolution and compound formation; in the most complex systems, both mechanisms are robustly present. The physical domain of the theoretical problem lies between the S/L interface from below and the L/V interface from above. A reasonable approximation to the L/V interfacial shape, based on the smallness of the Bond number Bo, is that of a spherical cap, an approximation validated by experimental observation in the absence of oxidation effects. No such simple approximation is valid for the S/L interface, whose dynamics are much more complex. The Hele–Shaw reactive wetting experiments reported here advance the state of knowledge of the dynamics of this interface. High speed videography of these experiments provides the first evidence that, following the initiation of wetting, a comparatively short time interval exists in which the S/L interface remains morphologically unchanged by the wetting process on a macroscopic length scale. A reactive wetting/spreading regime follows this early time regime in which the S/L interface can undergo first-order changes on macroscopic length scales due to both dissolution and the formation of compounds. In compound forming systems only, the reactive wetting/spreading regime can be followed by a kinetic roughening regime, characterized by growth of a solid phase in the contact line region which roughens an otherwise smooth contact line. We provide the first quantitative characterization of kinetic roughening for a high temperature system (Sn–Au/Cu) that reveals that certain similarities exist with kinetic roughening in room temperature systems (Hg–Au, Hg–Ag), in particular to the Hg–Ag system. We conjecture that the high temperature Sn–Au/Cu system belongs to the QKPZ universality class [21, 24, 27], however this conjecture should be confirmed by additional experiments. Finally, a fourth time regime exists, a long timescale on which the interfaces truly equilibrate by solid-state diffusion driven by curvature non-uniformities of the S/L interface. This regime requires years to complete and is inaccessible by practical experiments.

The existence of time regimes provides a potential rationale for theoretical investigation of the complete reactive wetting/spreading problem. In a sense, it poses the possibility that the end of each regime provides the initial conditions for the subsequent regime. The potential of the Hele–Shaw cell to elucidate the dynamics of the S/L interface is now clear, and should motivate follow-on theoretical (both analytical and computational) and additional experimental investigation of the reactive wetting/spreading problem in this configuration.

Acknowledgments

The authors would like to thank Dr Pavel Protsenko and colleagues for providing figure 3. The authors would also like to extend their gratitude to Dr Edmund Webb for his constructive comments on the manuscript. This work was supported by the National Science Foundation under grant DMR-0606408.

References

[1] de Gennes P G 1985 Wetting: statics and dynamics *Rev. Mod. Phys.* **57** 827
[2] Eustathopoulos N, Nicholas M G and Drevet B 1999 *Wettability at High Temperatures* (New York: Pergamon)
[3] Campbell C J, Fialkowski M, Bishop K J M and Grzybowski B A 2009 Mechanism of reactive wetting and direct visual determination of the kinetics of self-assembled monolayer formation *Langmuir* **25** 9–12
[4] Schultz W W, Worster M G and Anderson D M 2001 Solidifying sessile water droplets *Interactive Dynamics of Convection and Solidification* ed P Ehrhard, D S Riley and P H Steen (Dordrecht: Kluwer) pp 209–26
[5] Shiaffino S and Sonin A 1997 Molten droplet deposition and solidification at low Weber numbers *Phys. Fluids* **9** 3172
[6] Boettinger W J, Handwerker C A and Kattner U R 1993 Reactive wetting and intermetallic formation *The Mechanics of Solder Alloy Wetting and Spreading* ed F G Yost, F M Hosking and D R Frear (New York: Van Nostrand Reinhold) pp 103–39
[7] Dussan V E B 1979 On the spreading of liquids on solid surfaces: static and dynamic contact lines *Annu. Rev. Fluid Mech.* **11** 371
[8] Saiz E, Tomsia A P and Cannon R M 1998 Ridging effects on wetting and spreading of liquids on solids *Acta Mater.* **46** 2349
[9] Saiz E, Cannon R M and Tomsia A P 2000 Reactive spreading: adsorption, ridging and compound formation *Acta Mater.* **48** 4449
[10] Yin L, Meschter S J and Singler T J 2004 Wetting in the Au–Sn system *Acta Mater.* **52** 2873
[11] Yin L, Murray B T and Singler T J 2006 Dissolutive wetting in the Bi–Sn system *Acta Mater.* **54** 3561
[12] Yost F G and O'Toole E J 1998 *Acta Mater.* **46** 5143
[13] Warren J, Boettinger W and Roosen A 1998 Modeling reactive wetting *Acta Mater.* **46** 3247–64
[14] Su S, Yin L, Sun Y, Murray B T and Singler T J 2009 Modeling dissolution and spreading of Bi–Sn alloy drops on a Bi substrate *Acta Mater.* **57** 3110
[15] Yin L, Chauhan A and Singler T J 2008 Reactive wetting in metal/metal systems: dissolutive versus compound-forming systems *Mater. Sci. Eng.* A **495** 80
[16] Ockendon H and Ockendon J R 1995 *Viscous Flow* (Cambridge: Cambridge University Press)
[17] Erhardt P and Davis S H 1991 Non-isothermal spreading of liquid drops on horizontal plates *J. Fluid Mech.* **229** 365
[18] Protsenko P, Garandet J-P, Voytovych R and Eustathopoulos N 2009 submitted
[19] Rosenblat S and Davis S H 1985 How do liquid drops spread on solids *Frontiers of Fluid Mechanics* ed S H Davis and J L Lumley (Berlin: Springer) pp 171–83
[20] Kistler S F 1993 Hydrodynamics of wetting *Wettability* ed J C Berg (New York: Dekker) p 311
[21] Barabasi A L and Stanley H E 1995 *Fractal Concepts in Surface Growth* (Cambridge: Cambridge University Press)
[22] Be'er A, Hecht I and Taitelbaum H 2005 Interface roughening dynamics: temporal width fluctuations and the correlation length *Phys. Rev.* E **72** 031606
[23] Efraim Y 2008 *MSc. Thesis* Bar Ilan University Israel
[24] Efraim Y and Taitelbaum H 2009 Can Ising model and/or QKPZ equation properly describe reactive-wetting interface dynamics? *Cent. Eur. J. Phys.* **7** 503
[25] Be'er A, Lereah Y and Taitelbaum H 2008 Reactive-wetting of Hg–Ag system at room temperature *Mater. Sci. Eng.* A **495** 102
[26] Be'er A, Lereah Y, Frydman A and Taitelbaum H 2007 Spreading of mercury droplets on thin silver films at room temperature *Phys. Rev.* E **75** 051601
[27] Csahok Z, Honda K and Vicsek T 1993 Dynamics of surface roughening in disordered media *J. Phys. A: Math. Gen.* **26** L171
[28] Efraim Y and Taitelbaum H 2009 *Phys. Rev.* E submitted
[29] Be'er A, Lereah Y, Hecht I and Taitelbaum H 2001 The roughness and growth of a silver–mercury reaction interface *Physica* A **302** 297
[30] Be'er A, Lereah Y, Frydman A and Taitelbaum H 2002 Spreading of a mercury droplet on thin gold films *Physica* A **314** 325